Journal of Engineering Science and Technology
Vol. 13, No. 10 (2018) 3238 - 3251


# MULTISTATIC RADAR EMITTER IDENTIFICATION USING ENTROPY MAXIMIZATION BASED INDEPENDENT COMPONENT ANALYSIS

DILLIP DASH*, VALARMATHI J.

School of Electronics Engineering, VIT University, India
*Corresponding Author: dillipdash106@gmail.com

**Abstract**

Radar emitter identification is state-of-the-art in modern electronic warfare. Presently multistatic architecture is adapted by almost all the radar systems for better tracking performance and accuracy in target detection. Hence, identification and classification of radar emitters operating in the surveillance region are the major problems. To deal with the difficulty of identification of radar emitters in a complex electromagnetic environment, in this work entropy maximization method of Independent Component Analysis (ICA) based on gradient ascent algorithm is proposed. This algorithm separates unknown source signals from the interleaved multi-component radar signals. The discrete source signals are extracted from the multi-component signal by optimizing the entropy where maximum entropy is achieved using a gradient ascent approach through unsupervised learning. As better detection capability and range resolution are achieved by Linear Frequency Modulated (LFM) signals for radar systems here, multicomponent LFM signals with low SNR are considered as the signal mixture from which, the independent sources separated. A mathematical model of the algorithm for entropy maximization is illustrated in this paper. Simulation result validates the effectiveness of the algorithm in terms of time domain separation of the signal, and time-frequency analysis.

Keywords: Ambiguity function, Entropy maximization, Multicomponent signal, Multistatic radar.

## 1. Introduction

Radar emitter identification is a key problem in modern electronic reconnaissance system due to the current proliferation and waveform design complexity of electromagnetic signals [1]. Most of the radar system presently exploits multistatic architecture where the number of transmitter and receivers are more than one to improve the detection and tracking performance. As a result of this, a mixture of transmitting signal from all the transmitters is received by the receiver, which complicates the process of identifying the number of emitters operating in the surveillance region. It is also an important function of Electronic Countermeasures (ECM) of the modern electronic warfare to identify and locate the source of hostile radiations, based on analysing the intercepted radar signals. The conventional methods of emitter identification based on the received pulse parameter characteristics that is Time of Arrival (TOA), transmitted frequency of the signal, pulse duration, angle of arrival, pulse amplitude [2] and some parameters that are derived from the received pulse parameters like Pulse Repetition Interval (PRI) [3]. However, these algorithms became inefficient and time-consuming for solving emitter identification problems as they often fail to identify signals under high signal density environment, especially, in real time scenario [4].

Some of the researchers used in-pulse characteristics such as resemblance coefficient, wavelet package characteristic and complexity characteristic to recognising radar emitter. When signals have the same modulation type and different modulation parameters, these techniques cannot perform well. The modulating methods of intrapulse, inter-pulse are diverse and complicated [1]. Numerous pattern classification algorithms have been effectively implemented, like fuzzy functions [5], support vector machines [6], neural networks [7], and data association [8] by various authors. However, most of the available methods can accept only scalar input data and resolve the classification problem affected by the measurement ambiguity of the source feature parameters up to some level [9]. When the signal transmitted by multiple transmitters, the resultant echoes are a weighted sum of transmitted signals, which follow some type of distributions. In short, observation interval to classify the active emitters is one of the important task [10].

Radar emitter identification is a subclass of the broader data clustering problem, which aims to determine the unknown structure in a data set. However, compared to the common clustering problem, radar emitter identification has some distinctive challenges. Initially, radar data samples are of a large and irregular dimension may be of several hundreds of samples at a single scan and the other is that most of the pulses are very similar characteristics. Zhou and Lee [10] implemented offline clustering algorithms as a solution to the emitter classification problem. As stated by Liu et al. [11], these methods are effective, but in a practical scenario, online clustering algorithms are valuable, which is further considered, but it requires frequent training for satisfactory performance. Comon [12] firstly introduced the Independent Component Analysis (ICA) algorithm, intended for the blind source separation, for the application of radar emitter identification, which is presently reintroduced by researchers. Guo et al. [13] proposed a new emitter signal analysis method based on the complex ICA for multi-component LFM signal separation, which is a fixed-point algorithm with batch processing. A learning method based on Kernel Principal Component Analysis (KPCA) for emitter identification application consists of a symmetrical decomposition of the kernel matrix presented in [14]. As discussed by Yu et al. [15], identification of phase-coded radar sequence of the binary phase-coded radar signal is based on experimental model decomposition. Unintentional modulation refers to the characteristics of the detailed structure of a pulse. A Sequential Iterative Least Square (SILS) method, where iterative least square technique is employed for estimation of features in the cyclostationary domain and zero frequency slice of cyclic spectrum is explored in [16].

In this paper entropy maximization method of ICA is used to discretise the mixture of multicomponent LFM signals using unsupervised learning. This technique isolates unknown source signals from numerous signal mixtures by maximizing the entropy of a transformed set of signal mixtures. Here the Information maximization algorithm attains maximum entropy of a signal using gradient ascension, an iterative process of taking a step in the direction of maximum gradient until a local maximum is obtained. If this process is repeated sufficiently, the global maximum will reach. When the global maximum of entropy is found using gradient ascent, entropy has been maximized, and the resulting signals are the source signals. The following sections are organized as follows. Section 2 describes the multi-component signal modelling. Entropy maximization model is presented in Section 3. The gradient ascent approach is described in Section 4. Section 5 gives the simulation results and the conclusion is in Section 6.

## 2. Modelling of Multi-Component LFM Signal

In multistatic radar systems receiver frequently intercepts pulses, which are transmitted from different sources at the same time. As the pulse density increases, the interleaved pulses forms a multi-component signal. The signal model for multi-component LFM signal [17]:

$$s(t) = \sum_{i=0}^{S-1} A_i \mathrm{e}^{\mathrm{j}2\pi\left(\mathrm{f_i t}+\left(\mu_\mathrm{i} \mathrm{t}^2/2\right)\right)} + n(t) \quad (1)$$

where $S$ is the number of transmitters, $A_i$ is the absolute magnitude of each signal, $f_i$ is the initial frequency, $\mu_i$ is the chirp rate and $n(t)$ is the zero mean white Gaussian noise with variance $\sigma^2$. The mathematical representation of the signal mixture from which, the original signals has to extract is given by:

$$y = Wx \quad (2)$$

where $y$ is a vector that contains $M$ number of extracted source signals, $x$ is the mixture of $M$ signals and $W$ is the uncorrelated matrix. In vector matrix notation, it is represented by:

where $y$ is a vector that contains $M$ number of extracted source signals, $x$ is the mixture of $M$ signals and $W$ is the uncorrelated matrix. In vector matrix notation, it is represented by:

$$\begin{bmatrix} {y_1}^1 \, {y_1}^2 \cdots {y_1}^N \\ {y_2}^1 \, {y_2}^2 \cdots \, {y_2}^N \\ \vdots \quad \dots \quad \vdots \\ {y_M}^1 \, {y_M}^2 \, \cdots \, {y_M}^N \end{bmatrix} = \begin{bmatrix} W_{11} \, W_{12} \cdots W_{1M} \\ W_{21} \, W_{12} \cdots W_{2M} \\ \vdots \quad \vdots \quad \vdots \\ W_{M1} \;\; W_{M2} \cdots W_{MM} \end{bmatrix} \begin{bmatrix} {x_1}^1 \, {x_1}^2 \, \cdots {x_1}^N \\ {x_2}^1 \, {x_2}^2 \, \cdots {x_2}^N \\ \vdots \quad \vdots \quad \vdots \\ {x_M}^1 \, {x_M}^2 \, \cdots {x_M}^N \end{bmatrix} \quad (3)$$

The subscripts and superscripts of Eq. (3) indicate the signal number and the time index respectively. The extracted signal $y$ is obtained from the signal mixture $x$ by optimizing the separation matrix $W$.

## 3. Entropy Maximization Model

Entropy is the degree of uncertainty associated with an indiscriminate variable. Entropy (K) is the average information, which can be obtained for an arbitrary number of events $i$ by taking the expectation

$$K(A) = -\frac{1}{N}\sum_{t}^{N} ln\ P(A^t) \tag{4}$$

The entropy of mapped signal $Y$, can be represented mathematically by the entropy of a continuous random variable using Eq. (5), which becomes:

$$K(Y) = -\frac{1}{N}\sum_{t=1}^{N} \ln P_Y(Y^t) \tag{5}$$

Entropy maximization is one of the techniques of ICA, which aims to find the independent signals. The steps of the algorithm is described in Fig. 1. The entropy will be optimised by converting the mixed signals $y$ to another group of signals that is represented by:

$$Y = g(y) = g(\mathrm{Wx}) \tag{6}$$

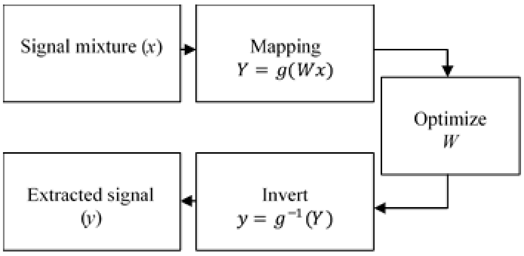


**Fig. 1. Entropy maximization algorithm block diagram.**

### 3.1. Uniformity of distribution and maximum entropy

Stone [17] describes entropy as a measure of uniformity of distribution such that complete uniformity equals maximum entropy. If $\boldsymbol{y}$ is a signal with cumulative distribution function (CDF) $g$, then the signal $Y = g(y)$ has maximum entropy and the probability density function (PDF) of $Y$ is uniform. Figure 2 shows how uniform distribution (A) is obtained after a signal (C) is transformed by its own CDF.

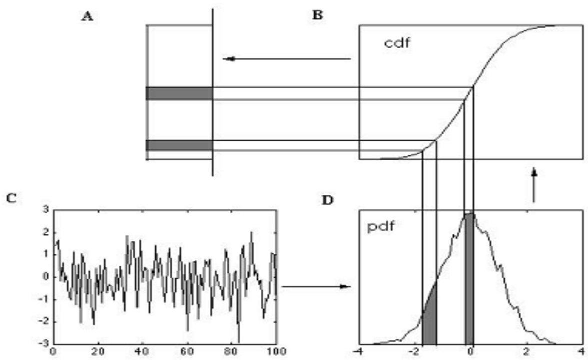


**Fig. 2. A uniform distribution (A) is obtained after a signal (C) is transformed by its own CDF [14].**

The PDF of the mapped signal $Y$ is $P_Y(Y^t)$ and the PDF of the extracted signal $y$ is $P_y(y^t)$. They are related as:

$$P_Y(Y^t)\, dY = P_y(y^t) dy \tag{7}$$

By removing the superscripts and rearranging the Eq. (7) yields:

$$P_Y(Y) = P_y(y)\, \frac{dy}{dY}$$

$$P_Y(Y^t) = \frac{P_y(y^t)}{\frac{dY}{dy}} = \frac{P_y(y^t)}{P_s(y^t)} \tag{8}$$

where $P_s(y^t)$ PDF of the source is signal and represented by $P_s(y^t) = \frac{dY}{dy}$.

Since $Y = g(y)$, where $g(y)$ is the model CDF of source signal then $\frac{dY}{dy} = g^{'}(y)$ and $g^{'}(y)$ is the PDF of the source signal. By substituting Eqs. (8) in (6), the entropy of the univariate PDF can be obtained as:

$$H(Y) = -\frac{1}{N}\sum_{t=1}^{N} ln\frac{P_y(y^t)}{P_s(y^t)} \tag{9}$$

Equation (9) provides a measure of similarity between the PDFs $P_y$ and $P_s$. If each extracted signal is transformed by a function $g$, then the joint distribution of the signal $\mathrm{y} = \mathrm{g(y)}$ is uniform at which, entropy is maximum. If an optimal separation matrix $w$ exists such that the extracted signals $\mathrm{y} = \mathrm{W}x$ have a joint PDF $P_y(y)$= $P_s(y)$.

$$P_Y(Y) = \frac{P_y(y)}{\left|\frac{\partial Y}{\partial y}\right|} \tag{10}$$

The denominator term is the Jacobean, which is a scalar value and is the determinant of a $M \times M$ jacobian matrix of the partial derivatives. Alternatively, Eq. (10) can be written as:

$$P_Y(Y) = \frac{P_y(y)}{P_s(y)} \tag{11}$$

By substituting Eqs. (11) in (9), results in the multivariate expression of the entropy in form of both the source signal PDF $P_s(y)$ and extracted signal PDF $P_y(y)$:

$$H(Y) = -\frac{1}{N}\sum_{t=1}^{N} ln\frac{P_y(y^t)}{P_s(y^t)} \tag{12}$$

$W$ is the separation matrix exists that maximizes the entropy of the signal $(Y) = g(y)$, the PDF $P_y$ of each extracted signal in $y = Wx$ will match to the PDF $P_s$. The function $P_s$ is used to specify the PDF of extracted signals because of the $W$, that maximizes the entropy. The mapping of $y = Wx$ leads to:

$$P_Y(y) = \frac{P_x(x)}{\left|\frac{\partial y}{\partial x}\right|} = \frac{P_x(x)}{|W|} \tag{13}$$

where $\frac{\partial y}{\partial x} = |W|$, and $P_Y(y)$ is PDF of the extracted signal.

### 3.2. Information maximization for entropy

On the substitution of Eqs. (13) in (12), the new expression for the multivariate entropy will be:

$$K(Y) = -\frac{1}{N}\sum_{t=1}^{N} ln \frac{P_x(x^t)}{|W|P_s(y^t)} \tag{14}$$

By applying the logarithmic properties, Eq. (14) is drafted as:

$$K(Y) = -\frac{1}{N}\sum_{t=1}^{N}(ln(P_x(x^t) - ln|W| - lnP_s(y^t))$$
$$= -\frac{1}{N}\sum_{t=1}^{N} ln(P_x(x^t) + \frac{1}{N}\sum_{t=1}^{N} ln|W| + lnP_s(y^t) \tag{15}$$

The first part of (15) is the entropy of the mixture signal $K(x)$. Equation (15) can be rewritten as:

$$K(Y) = K(x) + \frac{1}{N}\sum_{t=1}^{N} lnP_s(y^t) + ln|W| \tag{16}$$

From Eq. (16), we can say that the separation matrix $W$ that maximizes the entropy $K(Y)$ having no effect on $H(x)$. Therefore, in the next step, we can ignore $K(x)$. Then Eq. (16) can be modified as:

$$k(Y) = \frac{1}{N}\sum_{t=1}^{N} ln\ P_s(y^t) + ln|W| \tag{17}$$

In a modified form with $M$signal mixtures, it can be represented as:

$$k(Y) = \frac{1}{N}\sum_{i=1}^{M}\sum_{t=1}^{N} ln\ P_s({y_i}^t) + ln|W| \tag{18}$$

The parameter $W$ in Eq. (18) maximizes the entropy $Y$. As $y$ is the reverse of $Y$, that indicates the rows of $y$ are independent, which implies that $W$ is the separation matrix, which gives the original signals.

## 4. Gradient Ascent Approach

According to LeBlanc et al. [18], the gradient ascent method describes how to find the maximum point along a single curve that can be generalized to find the maximum point on a hill. The entropy of $Y$ is maximized by the separation matrix and for the optimization Gradient ascent method is used. Basically, gradient ascent is an iterative process of taking a step in the direction of maximum gradient until it approaches to a confined maximum.

### 4.1. Entropy gradient

The gradient of the entropy can be rewritten by taking the expectation over time of Eq. (18), which results:

$$k(Y) = E\{\sum_{i=1}^{M} ln\ P_s(y_i)\} + ln|W| \tag{19}$$

By calculating the partial derivative of $k$ with respect to $W$, the gradient is represented as:

$$\frac{\partial k(Y)}{\partial W_{ij}} = E\left\{\sum_{i=1}^{M}\frac{\partial \ln g'(y_i)}{\partial W_{ij}}\right\} + \frac{\partial ln|W|}{\partial W_{ij}} \tag{20}$$

$$\frac{\partial \ln g'(y_i)}{\partial W_{ij}} = E\left\{\sum_{i=1}^{M}\frac{g''(y_i)}{g'(y_i)}x_j\right\} \tag{21}$$

$$\frac{\partial ln|W|}{\partial W_{ij}} = [W^{-T}]_{ij} \quad (22)$$

On simplification of the first term and the second term of the partial derivative of Eq. (20) is given in Eqs. (21) and (22) respectively. Let assume one variable $\Psi(y_i)$ for simplification, that is:

$$\Psi(y_i) = \frac{g''(y_i)}{g'(y_i)}$$

Then the solution of the gradient of the entropy of Eq. (19) is given by:

$$\frac{\partial k(Y)}{\partial W_{ij}} = E\left\{\sum_{i=1}^{M} \Psi(y_i)\, x_j\right\} + [W^{-T}]_{ij} \quad (23)$$

The gradient of entropy $\nabla h$ for every element of the separation matrix $W$ is then:

$$\nabla k = W^{-T} + E\{\Psi(y)x^T\} \quad (24)$$

By generalizing the Eq. (24), the expression for the gradient of entropy $\nabla h$ is given by:

$$\nabla k = W^{-T} + \frac{1}{N}\sum_{t=1}^{N} \Psi(y^t)[x^t]^T \quad (25)$$

## 4.2. Gradient ascent technique for information maximization

The optimal separation matrix $W$ is found by maximizing the entropy that is iteratively following the gradient $\nabla k$ until it touches the local maximum. This is accomplished by

$$W_{updt} = W_{prev} + \eta \nabla k \quad (26)$$

where $\eta$ is a small positive constant. By putting the value of $\nabla k$ from Eq. (25) in Eq. (26), the updated weight value for which, the entropy is maximum is represented as:

$$W_{up} = W_{prv} + \eta\left({W_{prv}}^{-T} + \frac{1}{N}\sum_{t=1}^{N} \Psi(y^t)[x^t]^T)\right) \quad (27)$$

## 5. Simulation Results and Analysis

In the simulation, signal mixture one component, two component and three component independent LFM signals with noise are considered. In order to verify the validation of the proposed algorithm the extracted signals are analysed in terms of time domain separation (correlation coefficient), kurtosis maximization and Ambiguity function. The noise included is considered to be Gaussian in nature.

As expressed by Tsao et al. [19], Kurtosis, the fourth-order cumulant, can be considered as a measure indicating non-Gaussianity of a zero-mean random variable.

$$kurt(X) = \frac{E\{X^4\}}{(E\{X^2\})} - 3 \quad (28)$$

## 5.1. Time domain separation of a multi-component LFM signal

The time domain separation of the noise-corrupted multicomponent received radar signal is shown in this section. The original source signal, signal mixtures and the separated source signals are shown in a first, second and third row respectively in figures.

The signal extraction in an SNR of 10 dB of the one component, two component and multicomponent LFM signals with different mixing models are shown. Figure 3 represents the time domain separation of a single component LFM signal extracted from the mixture of Gaussian noise and the source signal and Table 1 gives the correlation coefficient values by correlating the source and extracted signal and the kurtosis values of the source and extracted signals are compared.

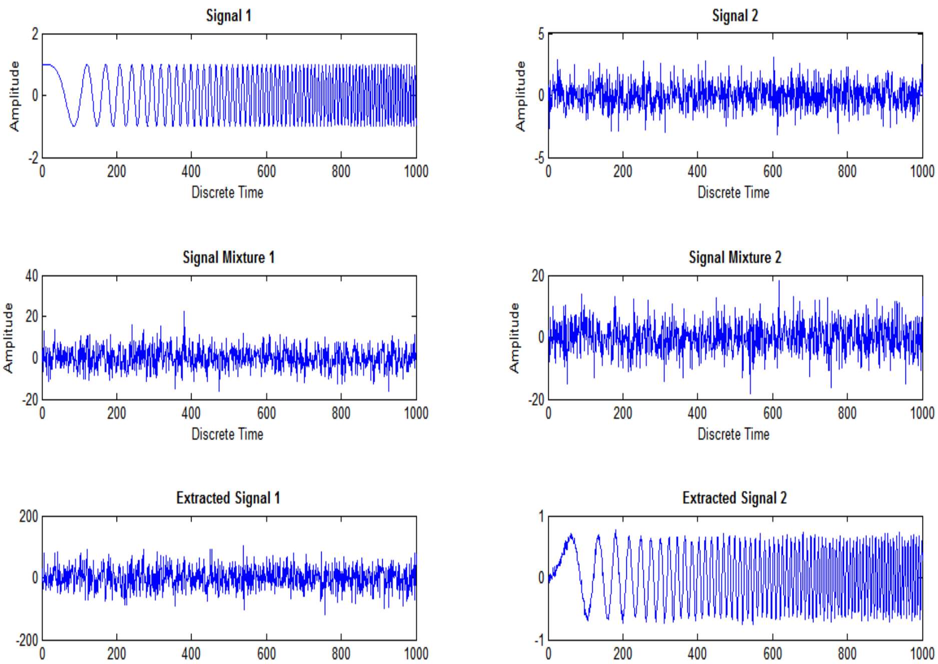


**Fig. 3. Single LFM signal separation from noise.**

**Table 1. Correlation coefficient and kurtosis of two signal mixture.**

| | **Correlation coefficient** | | **Kurtosis** | | |
|---|---|---|---|---|---|
| | **Extracted signal 1** | **Extracted signal 2** | **Source signal** | 15.10 | 3.242 |
| **Source signal 1** | 0.02 | **0.92** | **Observed signal** | 4.011 | 3.627 |
| **Source signal 2** | **0.86** | 0.018 | **Extracted Signal** | 15.01 | 3.261 |

Separation of the two components LFM with a convolutive mixture model and random mixing model are shown in Figs. 4 and 5 respectively. In the convolutive mixture model two source LFM signals are mixed with Gaussian noise and in the random mixing matrix model, two independent source LFM signals are mixed for the interleaved signal. The extracted signals are compared in terms of correlation coefficient and kurtosis is given in Tables 2 and 3.

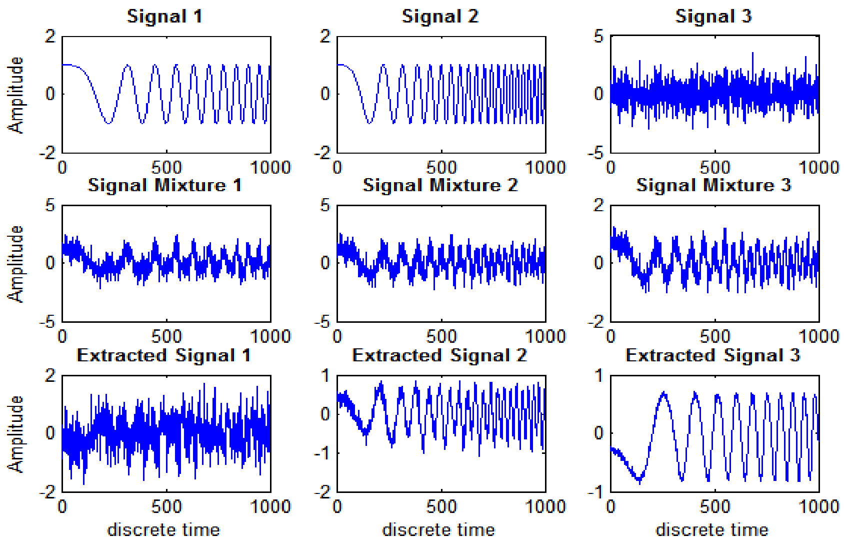


**Fig. 4. Multicomponent LFM signal separation from noise (convolutive mixture).**

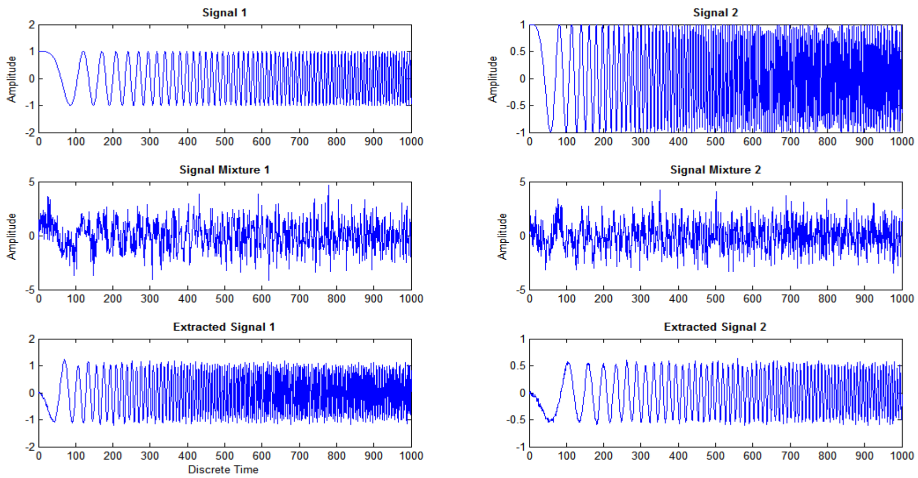


**Fig. 5. Multicomponent LFM signal separation from noise (random mixture).**

**Table 2. Correlation and Kurtosis of three signal mixture with noise.**

| | Correlation coefficient ($\rho$) | | | | Kurtosis | | |
|---|---|---|---|---|---|---|---|
| | **Extracted signal 1** | **Extracted signal 2** | **Extracted signal 3** | | **Signal 1** | **Signal 2** | **Signal 3** |
| **Source signal 1** | 0.04 | 0.25 | **0.92** | **Source signal** | 15.20 | 17.40 | 3.012 |
| **Source signal 2** | 0.06 | **0.90** | 0.28 | **Observed signal** | 4.991 | 3.789 | 5.211 |
| **Source signal 3** | **0.84** | 0.02 | 0.17 | **Extracted signal** | 3.112 | 15.36 | 16.98 |

**Table 3. Correlation and Kurtosis of three signal mixture without noise.**

| | Correlation coefficient ($\rho$) | | | | Kurtosis | | |
|---|---|---|---|---|---|---|---|
| | **Extracted signal 1** | **Extracted signal 2** | **Extracted signal 3** | | **Signal 1** | **Signal 2** | **Signal 3** |
| **Source signal 1** | **0.94** | 0.32 | 0.34 | **Source signal** | 15.86 | 16.27 | 15.65 |
| **Source signal 2** | 0.26 | **0.93** | 0.36 | **Observed signal** | 2.961 | 2.748 | 2.821 |
| **Source signal 3** | 0.29 | 0.29 | **0.91** | **Extracted signal** | 15.84 | 16.12 | 15.61 |

Three component LFM signal time domain separation is shown in Fig. 6, where the three independent LFM signals are mixed by random mixing matrix. Based on the entropy maximization criteria of the proposed algorithm, the three LFM signals are separated. The independence of the extracted signals is achieved by comparing the kurtosis of the source and extracted signals and in terms of the correlation coefficient, which is given in Table 4.

As entropy maximized, the gradient of entropy reduces and the plot of step size changes signifies the learning of gradient ascent algorithm. The parameter values assumed in this simulation are given in Table 5. The gradient ascent function values for the entropy, gradient of entropy and the step size are shown in first, second and third plots of Fig. 7. The entropy value converges after approximately 20 iterations.

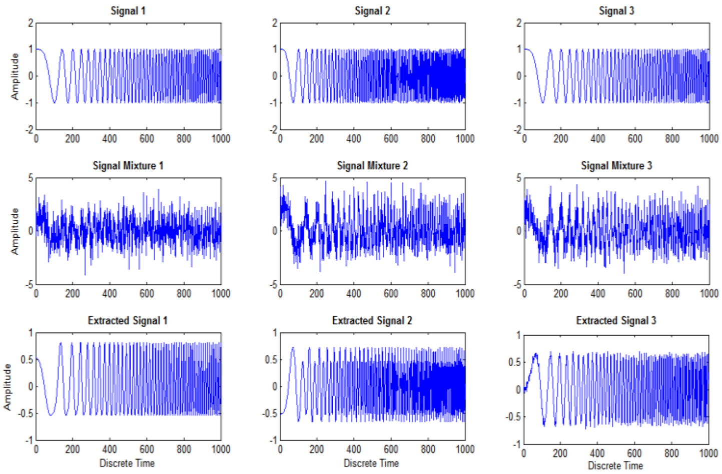


**Fig. 6. Multicomponent LFM signal separation from noise.**

**Table 4. Correlation and Kurtosis of two signal convolutive mixture with noise.**

| | Correlation coefficient | | Kurtosis | | |
|---|---|---|---|---|---|
| | **Extracted signal 1** | **Extracted signal 2** | **Source signal** | 14.82 | 16.01 |
| **Source signal 1** | 0.32 | **0.93** | **Observed signal** | 2.201 | 2.401 |
| **Source signal 2** | **0.92** | 0.34 | **Extracted signal** | 15.86 | 14.85 |

**Table 5. Parameter values.**

| | |
|---|---|
| **Number of repetitions** | 100 |
| **Initial step size** | 0.2 |
| **Step size increment factor** | 1.4 |
| **Step size decrement factor** | 0.1 |
| **Gradient ascent iterations** | 5 |

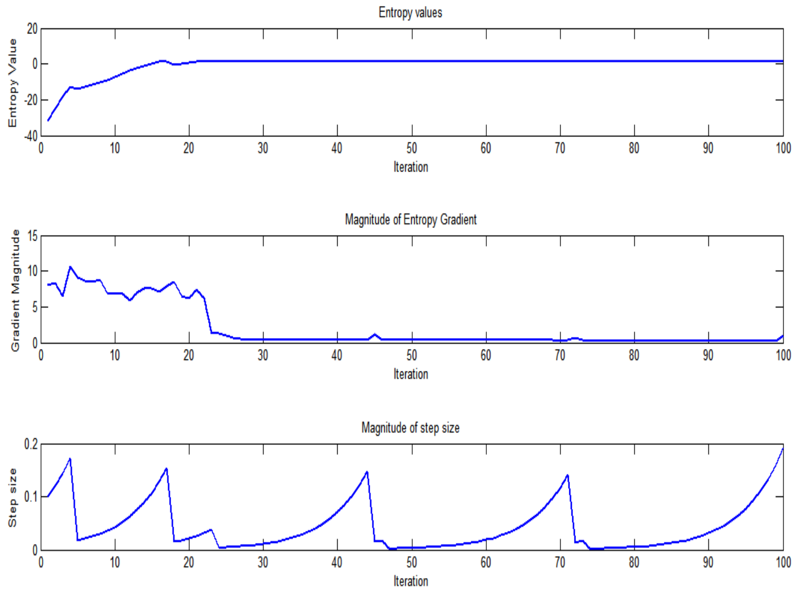


**Fig. 7. Entropy value, gradient magnitude and step size for gradient ascent repetitions.**

### 5.2. Time-frequency domain representation (ambiguity function)

In this section, the extracted signals from the signal mixtures are analysed in terms of the time-frequency domain, i.e., ambiguity functions. The ambiguity function plays an important role in radar waveform design and analysis. Basically, in radar applications AF $|\chi(\tau,\nu)|$ is the represention of resultant of the matched filter when the signal receives with a time delay $(\tau)$ and Doppler shift $(\nu)$ relative to the nominal values [16]. In mathematical form, it is represented by:

$$|\chi(\tau,\nu)| = \left|\int_{-\infty}^{\infty} r(t)r^*(t+\tau)e^{j2\pi\nu t}\ dt\right| \tag{29}$$

where $r(t)$ is the transmitted signal, $r^*(t+\tau)$ is conjugate of the received signal with delay $\tau$ and Doppler shift $\nu$. The ambiguity function of the LFM signal represents a central peak and the remaining energy distributed through the delay Doppler plane. The lack of any secondary peak in the ambiguity diagram signifies there is no range or Doppler ambiguity.

The matched filter response of the original LFM and extracted LFM signals are shown in Figs. 8 and 9. In this simulation, the LFM signal frequency and Doppler are considered as 20 MHz and 3 milliseconds respectively. It has been observed from the figure that the extracted signal response is having approximately similar parameters as compared to the original signal with energy concentrated in the single central peak.

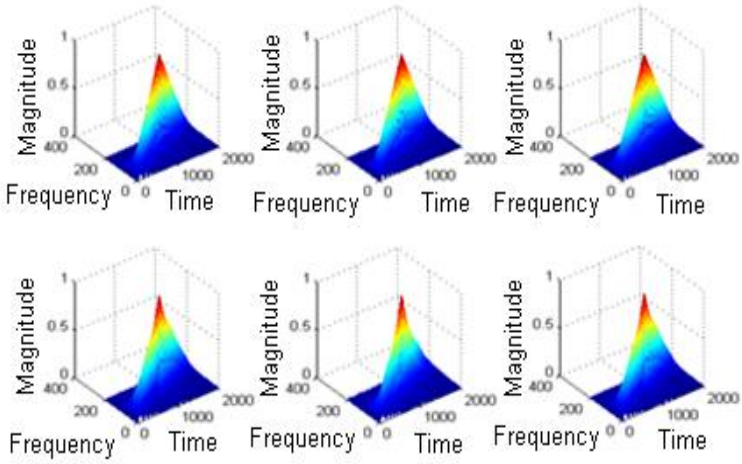


**Fig. 8. Ambiguity function of original and extracted LFM signal.**

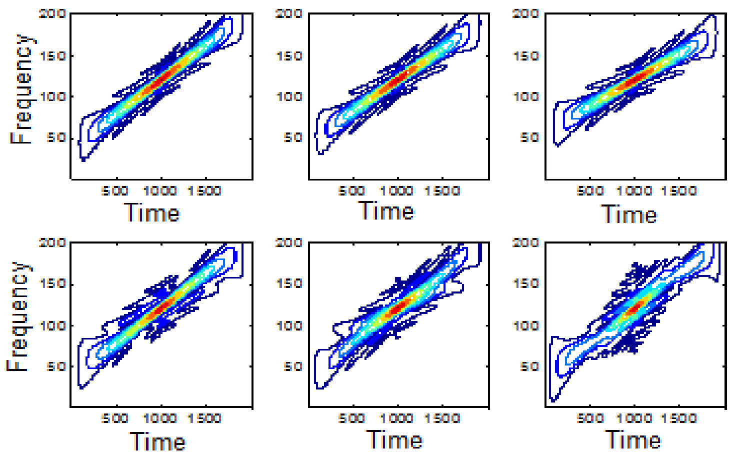


**Fig. 9. Ambiguity (contour) of the original and extracted LFM signal.**

## 6. Conclusion

In this paper, a classification technique based on independent component analysis for multi-component radar emitter signals in a multistatic radar system is proposed. The entropy of the signal is maximized through multiple iterations of the gradient ascent algorithm using an unsupervised learning rule. The time domain decomposition of the multi-component LFM signals from the various signal mixture are shown for different models and the extracted signals from the mixture are analysed in the time-frequency domain. This technique is quite effective to take out a trivial number of the separated signals from the equal number of signal combinations, but complex ground clutter does not consider in the signal transmission model. The impact of ground clutter and number of transmitters with complex models on the multicomponent LFM signal should be researched further.

**Nomenclatures**

| | |
|---|---|
| $E\{\}$ | Expectation operation |
| $kurt$ | Kurtosis |
| $n(t)$ | Gaussian noise |
| $Ps$ | PDF of the source signal |
| $Py$ | PDF of the extracted signal |
| $r(t)$ | Received signal |
| $S$ | Source signal |
| $W$ | Separation matrix |
| $\chi(\tau, \upsilon)$ | Ambiguity function |

***Greek Symbols***

| | |
|---|---|
| $\nabla_k$ | Gradient |
| $\eta$ | Constant |
| $\mu_i$ | Chirp rate of the LFM signal |
| $\tau$ | Delay of the received signal |
| $\upsilon$ | Doppler shift |

**Abbreviations**

| | |
|---|---|
| ECM | Electronic Counter Measure |
| LFM | Linear Frequency Modulation |
| TDOA | Time Difference of Arrival |
| TOA | Time of Arrival |

## References


1. Zhu, M.; Fu, K.; Huang, X.; Wu, S.; and Jin, W. (2013). A novel recognition approach for radar emitter signals based on on-line independent support vector machines. *Advances in Computer Science and its Applications*, 2(3), 390-396.
2. Ray, P.S. (1998). A novel pulse TOA analysis technique for radar identification. *IEEE transactions on Aerospace and Electronic Systems*, 34(3), 716-721.
3. Nishiguchi, K.; and Kobayashi, M. (2000). Improved algorithm for estimating pulse repetition intervals. *IEEE Transactions on Aerospace and Electronic Systems*, 36(2), 407-421.
4. Shieh, C.-S.; and Lin, C.-T. (2002). A vector neural network for emitter identification. *IEEE Transactions on Antennas and Propagation*, 50(8), 1120-1127.
5. Chen, Y.M.; Lin, C.-M.; and Hsueh, C.-S. (2014). Emitter identification of electronic intelligence system using type-2 fuzzy classifier. *Systems Science & Control Engineering: An Open Access Journal*, 2(1), 389-397.
6. Liu, Q. (2014). A novel radar emitters scheme recognition algorithm using support vector machine (SVM). *Information Technology Journal*, 13(4), 725-729.

7. Granger, E.; Rubin, M.A.; Grossberg, S.; and Lavoie, P. (2001). A what-and-where fusion neural network for recognition and tracking of multiple radar emitters. *Neural Networks*, 14(3), 325-344.
8. Liu, J.; Meng, H.; Liu, Y.; and Wang, X. (2010). Deinterleaving pulse trains in unconventional circumstances using multiple hypothesis tracking algorithm. *Signal Processing*, 90(8), 2581-2593.
9. Ata'a, A.W.; and Abdullah, S.N. (2007). Deinterleaving of radar signals and PRF identification algorithms. *IET Radar, Sonar & Navigation*, 1(5), 340-347.
10. Zhou, Y.; and Lee, J.P.Y. (1999). A MDL approach for determining the number of emitters using intra-pulse information. *Proceedings of the Conference on Communications, Computers and Signal Processing (PACRIM 1999).* Victoria, British Columbia, Canada, 548-551.
11. Liu, J.; Lee, J.P.; Li, L.; Luo, Z.Q.; and Wong, K.M. (2005). Online clustering algorithms for radar emitter classification. *IEEE Transactions on Pattern Analysis and Machine Intelligence*, 27(8), 1185-1196.
12. Comon, P. (1994). Independent component analysis, a new concept? *Signal Processing*, 36(3), 287-314.
13. Guo, Q.; Li, Y.; and Wang, C. (2011). A new method of detecting multi-component LFM signals based on blind signal processing. *Journal of Computers*, 6(9), 1976-1982.
14. Xu, D.; Yang, B.; Jiang, W.; and Zhou, Y. (2008). An improved SVDU-IKPCA algorithm for specific emitter identification. *Proceedings of the IEEE International Conference on Information and Automation*. Changsa, China, 692-696.
15. Yu, Z.; Jin, W.; Chen, C.; and Chen, T. (2008). Binary phase-coded sequence recognition based on EMD. *Proceedings of IEEE Congress in Image and Signal Processing*. Sanya, Hainan, China, 28-32.
16. Li, L.; and Ji, H. (2011). Radar emitter recognition based on cyclostationary signatures and sequential iterative least square estimation. *Expert Systems with Applications*, 38(3), 2140-2147.
17. Stone, J.V. (2005). Independent component analysis. Chichester, United Kingdom: John Wiley & Sons, Ltd.
18. LeBlanc, J.P.; and De Leon, P.L. (1998). Speech separation by kurtosis maximization. *Proceedings of the IEEE Conference on Acoustics, Speech and Signal Processing (ICASSP'98)*. Seattle, Washington, United States of America, 1029-1032 (Volume 2).
19. Tsao, T.; Slamani, M.; Varshney, P.; Weiner, D.; Schwarzlander, H.; and Borek, S. (1997). Ambiguity function for a bistatic radar. *IEEE Transactions on Aerospace and Electronic Systems*, 33(3), 1041-1051.